
On Characterizing and Mitigating Imbalances in Multi-Instance Partial Label Learning

Kaifu Wang

University of Pennsylvania
kaifu@sas.upenn.edu

Efthymia Tsamoura

Samsung AI
efi.tsamoura@samsung.com

Dan Roth

University of Pennsylvania
danroth@seas.upenn.edu

Abstract

Multi-Instance Partial Label Learning (MI-PLL) is a weakly-supervised learning setting encompassing *partial label learning*, *latent structural learning*, and *neurosymbolic learning*. Differently from supervised learning, in MI-PLL, the inputs to the classifiers at training-time are tuples of instances \mathbf{x} , while the supervision signal is generated by a function σ over the gold labels of \mathbf{x} . The gold labels are hidden during training. In this paper, we focus on characterizing and mitigating *learning imbalances*, i.e., differences in the errors occurring when classifying instances of different classes (aka *class-specific risks*), under MI-PLL. The phenomenon of learning imbalances has been extensively studied in the context of long-tail learning; however, the nature of MI-PLL introduces new challenges. Our contributions are as follows. From a theoretical perspective, we characterize the learning imbalances by deriving class-specific risk bounds that depend upon the function σ . Our theory reveals that learning imbalances exist in MI-PLL even when the hidden labels are uniformly distributed. On the practical side, we introduce a technique for estimating the marginal of the hidden labels using only MI-PLL data. Then, we introduce algorithms that mitigate imbalances at training- and testing-time, by treating the marginal of the hidden labels as a constraint. The first algorithm relies on a novel linear programming formulation of MI-PLL for pseudo-labeling. The second one adjusts a model’s scores based on robust optimal transport. We demonstrate the effectiveness of our techniques using strong neurosymbolic and long-tail learning baselines, discussing also open challenges.

1 Introduction

The need to reduce labeling cost motivates the study of weakly-supervised learning settings [59, 57]. Our work aligns with this objective, focusing on *multi-instance partial label learning* (MI-PLL) [49]. MI-PLL is particularly appealing, as it encompasses three well-known learning settings in the relevant literature: *partial label learning* (PLL) [17, 7, 3, 23, 37, 52, 54, 56, 47, 13], where each training instance is associated with a set of candidate labels, *latent structural learning* [40, 34, 58], i.e., learning classifiers subject to a transition function σ that constraints the classifiers’ outputs, and *neurosymbolic learning* [24, 51, 9, 43, 15, 20], i.e., training neural classifiers subject to symbolic background knowledge. An MI-PLL example is illustrated below:

Example 1.1 (MI-PLL example). *We aim to learn an MNIST classifier f , using only samples of the form (x_1, x_2, s) , where x_1 and x_2 are MNIST digits and s is the maximum of their gold labels, i.e., $s = \sigma(y_1, y_2) = \max\{y_1, y_2\}$ with y_i being the label of x_i . The gold labels are hidden during training. We will refer to the y_i ’s and s as hidden and partial labels, respectively.*

In this paper, we address an unexplored topic in the context of MI-PLL: that of characterizing and mitigating *learning imbalances*. By learning imbalances we refer to major differences in the errors occurring when classifying instances of different classes (aka *class-specific risks*). Existing works

in supervised [28, 4] and weakly-supervised learning [47, 13] study imbalances under the prism of *long-tailed* (aka *imbalanced*) data: data in which instances of different classes occur with very different frequencies, [12, 14, 2].

However, those studies cannot characterize learning imbalances in MI-PLL. This is because of two phenomena caused by the transition function σ : (i) the partial labels can be imbalanced even if the hidden labels are uniformly distributed; and (ii) different partial labels have very different supervision powers. Let us illustrate the above via Example 1.1. Regarding (i), even if both y_1 and y_2 are uniform in $\{0, \dots, 9\}$, the partials are long-tail when each training sample is formed by independently drawing pairs of MNIST digits and applying σ on their gold labels. In that case, $s = 0$ occurs with probability $1/100$, while $s = 9$ occurs with probability $17/100$ in the training data. Regarding (ii), partial label 0 provides much stronger supervision than partial label 9: in the former case, we have direct supervision, as $s = 0$ implies $y_1 = y_2 = 0$; in contrast, $s = 9$ only implies that either $y_1 = 9$ and y_2 is any label in $\{0, \dots, 9\}$, or vice versa. Figure 1 demonstrates this phenomenon by showing the per-class classification accuracy across different training epochs when an MNIST classifier is trained as in Example 1.1 and the hidden labels are uniform. Hence, to faithfully characterise imbalances in MI-PLL from a theoretical perspective, we need to account for the impact of σ .

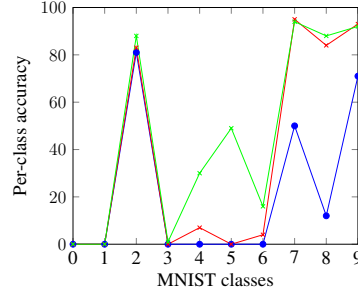


Figure 1: Accuracy of the classifier from Example 1.1. Blue, red and green curves show accuracy at 20, 40 and 100 epochs. Learning converges in 100 epochs.

On the practical side, mitigating learning imbalances has received considerable attention in supervised and weakly-supervised learning with the proposed techniques (typically referred to as *long-tail learning*) operating at training- [4, 42, 41, 6, 2] or at testing-time [18, 31, 28]. However, there are two main reasons that make those techniques not appropriate for MI-PLL. First, they rely on (good) approximations of the marginal distribution of the hidden labels. While approximating \mathbf{r} may be easy in supervised learning [28] as the gold labels are available, in our setting the gold labels are hidden from the learner. Second, the state-of-the-art for training-time mitigation [47, 4, 42, 41, 6, 2, 13] is designed for settings in which a single instance is presented each time to the learner and hence, they cannot take into account the correlations among the instances. The above gives rise to a second challenge: *developing techniques for mitigating learning imbalances in MI-PLL*.

Contributions. We start by providing class-specific error bounds in the context of MI-PLL. Complementary to previous work in supervised learning [4] and standard single-instance PLL [7], our theory shows that σ can have a significant impact on learning imbalances, capturing the phenomena (i) and (ii) described above, see Theorem 3.1. Our analysis also extends the theoretical analysis in [49], by providing stricter risk bounds for the underlying classifiers, while making minimal assumptions.

On the practical side, we first propose a statistically consistent technique for estimating the marginal of the hidden labels given partially labeled ones. We further propose two algorithms that mitigate imbalances at training- and testing-time, respectively. The first algorithm assigns pseudo-labels to training data based on a novel linear programming formulation of MI-PLL, see Section 4.2. The second algorithm aims to use the marginal information to constrain the model’s prediction on testing data, using a robust semi-constrained optimal transport (RSOT) formulation [19], see Section 4.3. Our empirical analysis demonstrates that our techniques can substantially improve the accuracy over strong baselines from neurosymbolic learning [53, 49] and long-tail learning [28, 13] by up to 14%, manifesting, at the same time, that the straightforward application of state-of-the-art techniques to MI-PLL settings is either impossible (e.g., [47]) or problematic (e.g., [13]). More importantly, our analysis uncovers open challenges for imbalance mitigation, that is *computing marginals for training-time mitigation* and *developing robust testing-time techniques*.

2 Preliminaries

Data and models. Let \mathcal{X} be the instance space and $\mathcal{Y} = \{l_1, \dots, l_c\}$ be the output space with $|\mathcal{Y}| = c$. The joint distribution of two random variables X, Y over $\mathcal{X} \times \mathcal{Y}$ is denoted as \mathcal{D} , with \mathcal{D}_X denoting the marginal of X . Vector $\mathbf{r} = (r_1, \dots, r_c)$ denotes the marginal of Y , where $r_j = \mathbb{P}(Y = l_j)$ is

the probability of occurrence (or ratio) of the j -th label. For a label $y = l_j (j \in [c])$, we express $r_y = r_{l_j} = r_j$. We consider *scoring functions* of the form $f : \mathcal{X} \rightarrow \Delta_c$, where Δ_c is the space of probability distributions on \mathcal{Y} , e.g., f outputs the softmax probabilities (or *scores*) of a neural classifier. We use $f^j(x)$ to denote the j -th output of $f(x)$. A scoring function f induces a *classifier* $[f] : \mathcal{X} \rightarrow \mathcal{Y}$, whose *prediction* on x is given by $f = \operatorname{argmax}_{j \in [c]} f^j(x)$. We denote by \mathcal{F} the set of scoring functions and by $[\mathcal{F}]$ the set of induced classifiers. The *zero-one loss* is given by $L(y', y) = \mathbb{1}\{y' \neq y\}$, while the *zero-one risk* of f is given by $R(f) := \mathbb{E}_{(X,Y) \sim \mathcal{D}}[L([f](X), Y)]$. Finally, the risk of f for the j -th class is defined as the probability of f mispredicting an instance of that class, i.e., $R_j(f) := \mathbb{P}([f](x) \neq l_j | Y = l_j)$. We refer to that risk as the *class-specific* one.

Multi-Instance PLL. We denote the vector (x_1, \dots, x_M) by \mathbf{x} and the corresponding vector of gold labels by \mathbf{y} . Let $\sigma : \mathcal{Y}^M \rightarrow \mathcal{S}$ be a transition function. Space $\mathcal{S} = \{a_1, \dots, a_{c_S}\}$ is referred to as *the partial label space* with $|\mathcal{S}| = c_S \geq 1$. We use $p_j = \mathbb{P}(S = a_j)$ to denote the probability of occurrence (or ratio) of the j -th partial label a_j . We assume that σ is known to the learner. Let \mathcal{T}_P be a set of m_P *partially labeled* samples of the form $(\mathbf{x}, s) = (x_1, \dots, x_M, s)$. Each partially labeled sample is formed by drawing M i.i.d. samples (x_i, y_i) from \mathcal{D} and then applying $s = \sigma(y_1, \dots, y_M)$. The distribution of these training samples (\mathbf{x}, s) is denoted by \mathcal{D}_P . For a classifier f , $[f](\mathbf{x})$ is a short for vector $([f](x_1), \dots, [f](x_M))$. The *zero-one partial loss subject to σ* is defined as $L_\sigma(\mathbf{y}, s) := L(\sigma(\mathbf{y}), s) = \mathbb{1}\{\sigma(\mathbf{y}) \neq s\}$, for any $\mathbf{y} \in \mathcal{Y}^M$ and $s \in \mathcal{S}$. We focus on learning via empirical risk minimization. In particular, the learner aims to find a classifier f with minimum *zero-one partial risk subject to σ* defined as $R_P(f; \sigma) := \mathbb{E}_{(X_1, \dots, X_M, S) \sim \mathcal{D}_P}[L_\sigma([f](\mathbf{X}), S)]$.

Vectors and matrices. $\mathbb{1}\{\cdot\}$ denotes indicator functions. For a integer $M \geq 0$, we define $[M] := \{1, \dots, M\}$. A vector is *diagonal* if all of its elements are equal. We denote by \mathbf{e}_i the vector with all its elements being equal to 0 apart from its i -th one which equals to 1. We denote the all-one and all-zero vectors in \mathbb{R}^n by $\mathbf{1}_n$ and $\mathbf{0}_n$, and the identity matrix of size $n \times n$ by \mathbf{I}_n . Let $\mathbf{A} \in \mathbb{R}^{n \times m}$ be a matrix. We use $A_{i,j}$ to denote the value of the (i, j) cell of \mathbf{A} and v_i to denote the i -th element of a vector \mathbf{v} . We denote the *vectorization* of \mathbf{A} by $\operatorname{vec}(\mathbf{A}) := [a_{1,1}, \dots, a_{n,1}, \dots, a_{1,m}, \dots, a_{n,m}]^\top$ and its *Moore–Penrose inverse* by \mathbf{A}^\dagger . If \mathbf{A} is square, then the diagonal matrix that shares the same diagonal with \mathbf{A} is denoted by $D(\mathbf{A})$. For matrices \mathbf{A} and \mathbf{B} , $\mathbf{A} \otimes \mathbf{B}$ and $\langle \mathbf{A}, \mathbf{B} \rangle$ denote their *Kronecker product* and their *Frobenius inner product*.

3 Theory: characterizing learning imbalances in MI-PLL

In this section, we characterize learning imbalances in MI-PLL from a theoretical perspective by deriving class-specific risk bounds, see Proposition 3.1. These bounds measure the difficulty of learning instances of each class in \mathcal{Y} , indicating that, unlike in supervised learning, imbalances in MI-PLL arise not only from label distribution imbalances but also from the partial labeling process. In particular, learning imbalances can still exist even if the hidden or the partial labels are uniformly distributed. Differently from prior work [49], our theoretical analysis relies solely on the i.i.d. assumption (see Section 2). To simplify our presentation, here we focus on the case where $M = 2$. Nevertheless, our analysis directly generalizes for $M > 2$.

Our theory is based on a novel non-linear programming formulation that allows us to compute an upper bound of each $R_j(f)$. The first key idea (K1) to that formulation is a rewriting of $R_P(f; \sigma)$ and $R_j(f)$. To start with, given the transition σ , the zero-one partial risk can be expressed as

$$R_P(f; \sigma) = \sum_{(l_i, l_j) \in \mathcal{Y}^2} \underbrace{r_i r_j}_{\text{probability of the pair } (l_i, l_j)} \left(\sum_{(l_{i'}, l_{j'}) \in \mathcal{Y}^2} \underbrace{\mathbb{1}\{\sigma(l_i, l_j) \neq \sigma(l_{i'}, l_{j'})\}}_{\text{the partial label is misclassified}} \underbrace{\mathbf{H}_{ii'}(f) \mathbf{H}_{jj'}(f)}_{\text{conditional probability that the labels } l_i \text{ and } l_j \text{ are (mis)classified as } l_{i'} \text{ and } l_{j'}} \right) \quad (1)$$

where $\mathbf{H}(f)$ is an $c \times c$ matrix defined as $\mathbf{H}(f) := [\mathbb{P}([f](x) = l_j | Y = l_i)]_{i \in [c], j \in [c]}$. In other words, the (i, j) cell in $\mathbf{H}(f)$ is the probability of f classifying (correctly or not) an instance with label l_i to l_j . Now, let $\mathbf{h}(f) = \operatorname{vec}(\mathbf{H}(f))$ be the vectorization of $\mathbf{H}(f)$. The partial risk $R_P(f; \sigma)$ in (1) is a quadratic form of $\mathbf{h}(f)$. Therefore, there is a unique symmetric matrix $\Sigma_{\sigma, \mathbf{r}}$ in $\mathbb{R}^{c^2 \times c^2}$ that depends only on σ and \mathbf{r} such that (1) can be rewritten as

$$R_P(f; \sigma) = \mathbf{h}(f)^\top \Sigma_{\sigma, \mathbf{r}} \mathbf{h}(f) \quad (2)$$

Furthermore, for each $l_j \in \mathcal{Y}$, let \mathbf{W}_j be the matrix defined by $(\mathbf{1}_c - \mathbf{e}_j)\mathbf{e}_j^\top$ and \mathbf{w}_j be its vectorization. We can rewrite the class-specific risk as

$$R_j(f) = \mathbf{w}_j^\top \mathbf{h}(f) \quad (3)$$

The second key idea (K2) to forming a non-linear program for computing class-specific risk bounds is to upper bound the class-specific risk $R_j(f)$ of a model f with the model’s partial risk $R_P(f; \sigma)$. The latter can be minimized with partially labeled data \mathcal{T}_P . Putting (K1) and (K2) together, the worst class-specific risk of f for the j -th class is given by the optimal solution of the program below:

$$\begin{aligned} \max_{\mathbf{h}} \quad & \mathbf{w}_j^\top \mathbf{h}(f) \\ \text{s.t.} \quad & \mathbf{h}(f)^\top \Sigma_{\sigma, \mathbf{r}} \mathbf{h}(f) = R_P(f; \sigma) && \text{(partial risk)} \\ & \mathbf{h}(f) \geq 0 && \text{(positivity)} \\ & (\mathbf{I}_c \otimes \mathbf{1}_c^\top) \mathbf{h}(f) = \mathbf{1}_c && \text{(normalization)} \end{aligned} \quad (4)$$

Let’s analyze (4). The optimization objective states that we aim to find the worst possible class-specific risk as expressed in (3). The first constraint specifies the partial risk of the model. The second one asks the (mis)classification probabilities to be non-negative. The last constraint, where $(\mathbf{I}_c \otimes \mathbf{1}_c^\top) \mathbf{h}(f)$ represents the row sums of matrix $\mathbf{H}(f)$, requires the classification probabilities to sum to one. Let $\Phi_{\sigma, j}(R_P(f; \sigma))$ denote the optimal solution to program (4). Formally, we have:

Proposition 3.1 (Class-specific risk bound). *For any $l_j \in \mathcal{Y}$, we have that $R_j(f) \leq \Phi_{\sigma, j}(R_P(f; \sigma))$.*

Characterizing learning imbalance. Theorem 3.1 suggests that the worst risk associated with each class in \mathcal{Y} is characterized by two factors. The first one is the model’s partial risk $R_P(f; \sigma)$, which is independent of the specific class. The second factor is σ , as σ impacts on the mapping $\Phi_{\sigma, j}$ from the model’s partial risk to the class-specific risk. Therefore, the learning imbalance can be assessed by comparing the growth rates of $\Phi_{\sigma, j}$. We use this approach below to analyze Example 1.1.

Example 3.2 (Cont’ Example 1.1). *Let \mathcal{D} and \mathcal{D}_P be defined as in Section 2. Consider the two cases:*

CASE 1 *The marginal of the hidden label Y is uniform. The left-hand side of Figure 2 shows the risk bounds for different classes obtained via solving program (4). The bounds are presented as functions of different values of $R_P(f; \sigma)$. In this plot, the curve for class “zero” (resp. “nine”) has the steepest (resp. smoothest) slope, suggesting that f will tend to make more (resp. fewer) mistakes when classifying instances of that class. In other words, class “zero” is the hardest to learn, as also shown to be the case in reality, see Figure 1.*

CASE 2 *The marginal of the partial label S is uniform. Similarly, the right-hand side Figure 2 plots the corresponding risk bounds, suggesting that the class “zero” is now the easiest to learn.*

Obtaining the label ratio \mathbf{r} .

Computing the program (4) requires knowing the transition σ and the label distribution \mathbf{r} . While σ is assumed to be given, \mathbf{r} may be unknown in practice. To circumvent this, in Section 4.1, we present a technique for estimating \mathbf{r} using only partially labeled data \mathcal{T}_P .

Computable bounds for $R_j(f)$.

Using Proposition 3.1, we could further derive a bound for $R_j(f)$ that can be computed using an MI-PLL dataset. This can be done by using standard learning theory tools (e.g., VC-dimension or Rademacher complexity) to show that, given a fixed confidence level $\delta \in (0, 1)$, the partial risk $R_P(f; \sigma)$ will not exceed a *generalization bound* $\tilde{R}_P(f; \sigma, \mathcal{T}_P, \delta)$ with probability $1 - \delta$. An example is shown below.

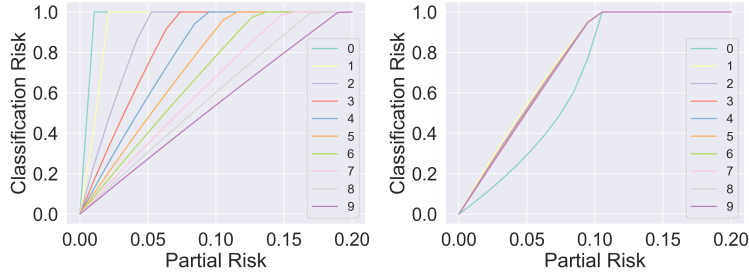


Figure 2: Class-specific upper bounds obtained via (4). (left) \mathcal{D}_Y is uniform. (right) \mathcal{D}_{P_S} is uniform.

Proposition 3.3. Let $d_{[\mathcal{F}]}$ be the Natarajan dimension of $[\mathcal{F}]$. Given a confidence level $\delta \in (0, 1)$, we have that $R_j(f) \leq \Phi_{\sigma,j}(\tilde{R}_{\mathcal{P}}(f; \sigma, \mathcal{T}_{\mathcal{P}}, \delta))$ with probability $1 - \delta$ for any $j \in [c]$, where

$$\tilde{R}_{\mathcal{P}}(f; \sigma, \mathcal{T}_{\mathcal{P}}, \delta) = \hat{R}_{\mathcal{P}}(f; \sigma, \mathcal{T}_{\mathcal{P}}) + \sqrt{\frac{2 \log(em_{\mathcal{P}}/2d_{[\mathcal{F}]}) \log(6Mc^2d_{[\mathcal{F}]} / e)}{m_{\mathcal{P}}/2d_{[\mathcal{F}]}} \log(6Mc^2d_{[\mathcal{F}]} / e)} + \sqrt{\frac{\log(1/\delta)}{2m_{\mathcal{P}}}} \quad (5)$$

Comparison to previous work. The most relevant work to ours is [49], which provides the first theoretical framework that establishes the learnability for MI-PLL. Our result extends [49] in three ways: (i) we bound the class-specific risks $R_j(f)$ instead of bounding the total risk $R(f)$; (ii) our bounds do not rely on M -unambiguity, in contrast to those in [49]; and (iii) the program (4) leads to tighter bounds for $R(f)$. Before proving (iii), let us first recapitulate M -unambiguity:

Definition 3.4 (M -unambiguity from [49]). A transition σ is M -unambiguous if for any two diagonal label vectors \mathbf{y} and $\mathbf{y}' \in \mathcal{Y}^M$ such that $\mathbf{y} \neq \mathbf{y}'$, we have that $\sigma(\mathbf{y}') \neq \sigma(\mathbf{y})$.

Now, let us illustrate (iii) from above. By relaxing the constraints in (4), we can recover Lemma 1 from [49] (which is the key to proving Theorem 1 from [49]). In particular, if we: (1) drop the positivity and normalization constraints from (4) and (2) replace the partial risk constraint by a more relaxed inequality $\mathbf{h}(f)^\top D(\Sigma_{\sigma, \mathbf{r}}) \mathbf{h}(f) \leq R_{\mathcal{P}}(f; \sigma)$, we can obtain the following result:

Proposition 3.5. If σ is M -unambiguous, then the risk of f can be bounded by

$$R(f) \leq \sqrt{\mathbf{w}^\top (D(\Sigma_{\sigma, \mathbf{r}})^\dagger) \mathbf{w} R_{\mathcal{P}}(f; \sigma)} = \sqrt{c(c-1) R_{\mathcal{P}}(f; \sigma)} \quad (6)$$

which coincides with the Lemma 1 from [49] for $M = 2$.

4 Algorithms: mitigating imbalances in MI-PLL

We now propose a portfolio of techniques for addressing learning imbalances in MI-PLL. Our first contribution, see Section 4.1, is a statistically consistent technique for estimating \mathbf{r} , assuming access to partial labels only. We then move to training-time mitigation, see Section 4.2 and testing-time mitigation, see Section 4.3. Our marginal estimation algorithm requires only the i.i.d. assumption of MI-PLL; the algorithms in Section 4.2 and 4.3 work even when the i.i.d. assumption fails to hold.

4.1 Estimating the marginal of the hidden labels

We begin with our technique for estimating \mathbf{r} using only partially labeled data $\mathcal{T}_{\mathcal{P}}$. Our technique for estimating \mathbf{r} relies on the observation that in MI-PLL, the ratio p_j of a partial label $a_j \in \mathcal{S}$ equals the probability of its pre-image $\sigma^{-1}(a_j)$, namely $p_j = \sum_{(y_1, \dots, y_M) \in \sigma^{-1}(a_j)} \prod_{i=1}^M r_{y_i}$, which is a polynomial of \mathbf{r} . We illustrate the above idea with the following example.

Example 4.1. Consider CASE (2) from Example 3.2. Assume that the marginals of the partial labels are uniform. Then, we can obtain \mathbf{r} via solving the following system of polynomial equations: $[r_0^2, r_1^2 + 2r_0r_1, \dots, r_9^2 + 2\sum_{i=0}^8 r_i r_9]^\top = [1/10, 1/10, \dots, 1/10]^\top$. The first equation denotes the probability a partial label to be zero, which is $1/10$ (uniformity). Due to σ , this can happen only when $y_1 = y_2 = 0$. Under the independence assumption, the above implies that $r_0^2 = 1/10$. Analogously, the second and the last polynomials denote the probabilities a partial label to be one and nine.

Let Ψ_σ be the mapping $\mathbf{r} \mapsto \mathbf{p} = [p_j]_{j \in [c_S]}$ as defined above. In practice, the marginal \mathbf{p} is unknown, but can be estimated by the empirical distribution of a partially labeled dataset $\mathcal{T}_{\mathcal{P}}$ of size $m_{\mathcal{P}}$, namely $\bar{p}_j := \sum_{k=1}^{m_{\mathcal{P}}} \mathbb{1}\{s_k = a_j\} / m_{\mathcal{P}}$. As the \bar{p}_j 's can be noisy, the system of polynomials could become inconsistent. Therefore, instead of solving the polynomial equation as in Example 4.1, we find an estimate $\hat{\mathbf{r}}$, so that its induced prediction for the partial label ratio $\hat{\mathbf{p}} := \Psi_\sigma(\hat{\mathbf{r}})$ best fits to the empirical probabilities \bar{p}_j 's by means of cross-entropy. Since this requires optimizing over the probability simplex Δ_c , we reparametrize the estimated ratios $\hat{\mathbf{r}}$ as $\hat{\mathbf{r}} = \text{softmax}(\mathbf{u})$, leading to Algorithm 1. We also provide a theoretical guarantee for the consistency of Algorithm 1 in Appendix C.

4.2 Training-time imbalance mitigation via integer linear programming

We now turn to training-time mitigation. We aim to find pseudo-labels \mathbf{Q} that are close to the classifier's scores and adhere to $\hat{\mathbf{r}}$ and use \mathbf{Q} to train the classifier using the cross-entropy loss. There

Algorithm 1 LABEL RATIO SOLVER

Input: partial labels $\{s_k\}_{k=1}^{mp}$, transition function σ , step size t , iterations N_{iter}
Initialize: logit $\mathbf{u} \leftarrow \mathbf{1}_c$; \bar{p}_j , for $j \in [c_S]$
for $N = 1, \dots, N_{\text{iter}}$ **do**
 $\hat{\mathbf{r}} \leftarrow \text{softmax}(\mathbf{u})$
for each $j \in [c_S]$ **do**
 $\hat{p}_j \leftarrow \sum_{(y_1, \dots, y_M) \in \sigma^{-1}(a_j)} \prod_{i=1}^M \hat{r}_{y_i}$
 $\ell \leftarrow \sum_{j=1}^{c_S} \bar{p}_j \log \hat{p}_j$
Backpropagate ℓ to update \mathbf{u}
return $\text{softmax}(\mathbf{u})$

Algorithm 2 CAROT

Input: model's raw scores $\mathbf{P} \in \mathbb{R}^{c \times n}$, ratio estimates $\hat{\mathbf{r}} \in \mathbb{R}^c$, entropic reg. parameter $\eta > 0$, margin reg. parameter $\tau > 0$, iterations N_{iter}
Initialize: $\mathbf{u} \leftarrow \mathbf{0}_n$; $\mathbf{v} \leftarrow \mathbf{0}_c$
for $N = 1, \dots, N_{\text{iter}}$ **do**
 $\mathbf{a} \leftarrow B(\mathbf{u}, \mathbf{v})\mathbf{1}_c$; $\mathbf{b} \leftarrow B(\mathbf{u}, \mathbf{v})^\top \mathbf{1}_n$
if k is even **then**
update \mathbf{v} //see Section 4.3
else
update \mathbf{u} //see Section 4.3
return $B(\mathbf{u}, \mathbf{v})$

are two design choices: (i) whether to find pseudo-labels at the individual instance level or at the batch level; (ii) whether to be strict in enforcing the marginal $\hat{\mathbf{r}}$. In addition, we face two challenges: (iii) we are provided with M -ary tuples of instances of the form (x_1, \dots, x_M) ; (iv) \mathbf{Q} must additionally abide by the constraints coming from σ and the partial labels, e.g., when $s = 1$ in Example 1.1, then the only valid label assignments for (x_1, x_2) are (1,1), (0,1) and (1,0). Regarding (i), finding pseudo-labels at the individual instance level does not guarantee that the modified scores match the desired distribution $\hat{\mathbf{r}}$ [31]. Regarding (ii), strictly enforcing $\hat{\mathbf{r}}$ could be problematic as $\hat{\mathbf{r}}$ can be noisy.

To accommodate the above requirements, while avoiding the crux of solving non-linear programs, we rely on a novel *linear programming* (LP) formulation of MI-PLL that finds pseudo-labels for a batch of n scores. Let us introduce our notation. We use $(x_{\ell,1}, \dots, x_{\ell,M}, s_\ell)$ to denote the ℓ -th partial training sample in a batch of size n . We also use $\mathbf{P}_i \in [0, 1]^{n \times c}$ and $\mathbf{Q}_i \in [0, 1]^{n \times c}$, for $i \in [M]$, to denote the classifier's scores and the pseudo-labels assigned to the i -th input instances of the batch. In particular, $P_i[\ell, j] = f^j(x_{\ell,i})$, while $Q_i[\ell, j]$ is the corresponding pseudo-label. Each training sample is uniquely associated with a Boolean formula of R_ℓ disjuncts of the form $\Phi_\ell = \varphi_{\ell,1} \vee \dots \vee \varphi_{\ell,R_\ell}$. Formula Φ_ℓ encodes the valid label assignments for the ℓ -th partial training sample subject to σ and s_ℓ and is exclusively determined by σ and s_ℓ . Each disjunct in Φ_ℓ is a conjunction of Boolean variables from $\{q_{\ell,i,j}\}_{i \in [M], j \in [c]}$, where $q_{\ell,i,j}$ is true if and only if $x_{\ell,i}$ is assigned to the j -th label in \mathcal{Y} . We assume a canonical ordering over the variables occurring in $\varphi_{\ell,t}$ and use $\varphi_{\ell,t,k}$ to refer to the k -th variable and $|\varphi_{\ell,t}|$ to denote the number of variables occurring in $\varphi_{\ell,t}$.

Based on the above, finding a pseudo-label assignment for $(x_{\ell,1}, \dots, x_{\ell,M})$ that adheres to σ and s_ℓ reduces to finding an assignment to the variables in $\{q_{\ell,i,j}\}_{i \in [M], j \in [c]}$ that makes Φ_ℓ hold. Previous work ([35, 39]) has shown that we can cast satisfiability problems (as the one above) to linear programming problems. Therefore, instead of finding a Boolean true or false assignment to each $q_{\ell,i,j}$, we can find an assignment in $[0, 1]$ for the real counterpart of $q_{\ell,i,j}$ denoted by $[q_{\ell,i,j}]$. Via associating the $[q_{\ell,i,j}]$'s to the entries in the \mathbf{Q}_i 's, i.e., $Q_i[\ell, j] = [q_{\ell,i,j}]$, we can solve the following linear program to perform pseudo-labeling:

$$\begin{aligned}
\text{objective} \quad & \min_{(\mathbf{Q}_1, \dots, \mathbf{Q}_M)} \sum_{i=1}^M \langle -\log(\mathbf{P}_i), \mathbf{Q}_i \rangle, \\
\text{s.t.} \quad & \sum_{t=1}^{R_\ell} [\alpha_{\ell,t}] \geq 1, & \ell \in [n] \\
& -|\varphi_{\ell,t}|[\alpha_{\ell,t}] + \sum_{k=1}^{|\varphi_{\ell,t}|} [\varphi_{\ell,t,k}] \geq 0, & \ell \in [n], t \in [R_\ell] \\
& -\sum_{k=1}^{|\varphi_{\ell,t}|} [\varphi_{\ell,t,k}] + [\alpha_{\ell,t}] \geq (1 - |\varphi_{\ell,t}|), & \ell \in [n], t \in [R_\ell] \\
& \sum_{j=1}^c [q_{\ell,i,j}] = 1, & \ell \in [n], i \in [M] \\
& [q_{\ell,i,j}] \in [0, 1], & \ell \in [n], i \in [M], j \in [c] \\
& |\mathbf{Q}_i \cdot \mathbf{1}_n - n\hat{\mathbf{r}}| \leq \epsilon, & i \in [M]
\end{aligned} \tag{7}$$

The minimization objective in (7) aligns with our aim to find pseudo-labels close to the classifier's scores. The independence among the classifier's scores for different $\mathbf{x}_{\ell,i}$'s— recall that a classifier makes a prediction for each $\mathbf{x}_{\ell,i}$ independently of the other instances— justifies the sum over different i 's in the minimization objective. The first three constraints force the pseudo-labels for the ℓ -th training sample to adhere to σ and s_ℓ , where the $\alpha_{\ell,t}$'s are Boolean variables introduced due to

converting the Φ_ℓ 's into *conjunctive normal form* using the Tseytin transformation [44]. The fourth and the fifth constraint wants the pseudo-labels for each instance $x_{\ell,i}$ to sum up to one and lie in $[0, 1]$. Finally, the last constraint wants for each $i \in [M]$, the probability of predicting the j -th pseudo-label for an element in $\{x_{\ell,i}\}_{\ell \in [n]}$ to match the ratio estimates at hand \hat{r}_j up to some $\epsilon \geq 0$: the smaller ϵ gets, the stricter the adherence to $\hat{\mathbf{r}}$ becomes. The detailed derivation of (7) is in the appendix.

To summarize, training-time mitigation works as follows: for each epoch, we split the training samples in \mathcal{T}_P into batches. For each batch $\{(x_{\ell,1}, \dots, x_{\ell,M}, s_\ell)\}_{\ell \in [n]}$, we form matrices $\mathbf{P}_1, \dots, \mathbf{P}_M$ by applying f on the $x_{\ell,i}$'s and solve (7) to get the pseudo-label matrices $\mathbf{Q}_1, \dots, \mathbf{Q}_M$. Finally, we train f by minimizing the cross-entropy loss between $\mathbf{Q}_1, \dots, \mathbf{Q}_M$ and $\mathbf{P}_1, \dots, \mathbf{P}_M$.

Remarks. Our formulation in (7) is oblivious to $\hat{\mathbf{r}}$. In particular, $\hat{\mathbf{r}}$ can be estimated using either Algorithm 1 from Section 4.1 or any other technique, such as the moving average one from [47]. Furthermore, the formulation in (7) allows us to find either hard or soft pseudo-labels: we can treat (7) as an integer linear program via enforcing $[q_{\ell,i,j}]$ to lie in $\{0, 1\}$, instead of $[0, 1]$.

4.3 CAROT: testing-time imbalance mitigation

We conclude this section with CAROT, an algorithm that mitigates learning imbalances at testing-time by modifying the model's scores to adhere to the estimated ratios $\hat{\mathbf{r}}$. Incorporating $\hat{\mathbf{r}}$ into the model's scores involves the design choices (i) and (ii) presented at the beginning of Section 4.2—challenges (iii) and (iv) are specific to training. Regarding (i), most existing testing-time mitigation algorithms (e.g., [28]) modify a model's scores at the level of individual instances. Regarding (ii), as we explained in Section 4.2, strictly enforcing $\hat{\mathbf{r}}$ could also be problematic, as now, $\hat{\mathbf{r}}$ may be also different from the label marginal underlying the test data.

Similarly to Section 4.2, we propose to adjust the model's scores for a whole batch of $n > 1$ test samples (represented by a matrix $\mathbf{P} \in \mathbb{R}^{n \times c}$) so that the adjusted scores \mathbf{P}' roughly adhere to $\hat{\mathbf{r}}$. Precisely, we propose to find \mathbf{P}' that optimizes the following objective:

$$\min_{\mathbf{P}' \in \mathbb{R}_+^{n \times c}, \mathbf{P}' \mathbf{1}_c = \mathbf{1}_n} \langle -\log(\mathbf{P}), \mathbf{P}' \rangle + \tau \text{KL}(\mathbf{P}'^T \mathbf{1}_n \parallel n\hat{\mathbf{r}}) - \eta H(\mathbf{P}') \quad (8)$$

The first term in (8) encourages \mathbf{P}' to be close to the original scores. The second term encourages the column sums of \mathbf{P}' to match $\hat{\mathbf{r}}$, with $\tau > 0$ controlling the level of adherence, where KL is the Kullback-Leibler divergence. This formulation leads to a *robust semi-constrained optimal transport* (RSOT) problem [19]. The entropic regularizer $\eta H(\mathbf{P}')$, where H denotes entropy, allows to approximate the optimal solution using the robust semi-Sinkhorn algorithm from [19], leading to CAROT (*Confidence-Adjustment via Robust semi-constrained Optimal Transport*), see Algorithm 2.

In Algorithm 2, $B(\mathbf{u}, \mathbf{v})$ denotes an $n \times c$ matrix whose (i, j) cell is computed as a function of \mathbf{u} and \mathbf{v} by $\exp(u_i + v_j + \log(P_{ij})/\eta)$. In each iteration, the algorithm alternates between updating the c -dimensional vector \mathbf{v} and the n -dimensional vector \mathbf{u} . The former update, which is computed as $\mathbf{v} \leftarrow \frac{\eta\tau}{\eta+\tau} \left(\frac{\mathbf{v}}{\eta} + \log(n\hat{\mathbf{r}}) - \log(\mathbf{b}) \right)$, forces $B(\mathbf{u}, \mathbf{v})$ to adhere to $\hat{\mathbf{r}}$; the latter one, which is computed as $\mathbf{u} \leftarrow \eta \left(\frac{\mathbf{u}}{\eta} + \log(\mathbf{1}_n) - \log(\mathbf{a}) \right)$, forces the elements in each row of $B(\mathbf{u}, \mathbf{v})$ to add to one. Matrix $B(\mathbf{u}, \mathbf{v})$ converges to the optimal solution to (8) when N_{iter} goes to infinity, as claimed in [19].

Choice of η and τ . In practice, we use a small *partially labeled* validation set to choose η and τ . Doing so, the validation set can be obtained by splitting the training set of partially labelled data \mathcal{T}_P .

5 Experiments

Baselines. We consider the state-of-the-art loss *semantic loss* (SL) [53, 49, 15] for MI-PLL training and use the engine Scallop that performs MI-PLL training using that loss [15]. Since there are no prior MI-PLL techniques for mitigating imbalances at testing-time, we consider Logit Adjustment (LA) [28] as a competitor to CAROT. The notation $+A$, for an algorithm $A \in \{\text{LA}, \text{CAROT}\}$, means that the scores of a baseline model are modified at testing-time via A . We do not assume access to a validation set of gold labelled data, applying LA and CAROT using the estimate $\hat{\mathbf{r}}$ obtained via Algorithm 1. However, we use a validation set of partially labelled data to run Algorithm 1. We also carry experiments with RECORDS [13], a technique that mitigates imbalances at training-time for standard PLL (again, no previous MI-PLL training-time baseline exists). We

use SL+RECORDS when a model has been trained using RECORDS in conjunction with SL. RECORDS acts as a competitor to our LP-based technique from Section 4.2. Notice that the imbalance mitigation technique from [47], SoLAR, cannot act as a competitor to our proposed techniques (see Section 6 and Appendix E for a detailed discussion on SoLAR). Finally, we carry experiments using our LP-based technique. We use LP(ALG1) and LP(EMP), when LP is applied using the estimate \hat{r} obtained via Algorithm 1 and via the approximation from [47], respectively.

Benchmarks. We carry experiments using an MI-PLL benchmark previously used in the neurosymbolic literature [24, 25, 15, 20], namely MAX- M , as well as a newly introduced, called Smallest Parent. Training samples in MAX- M are as described in Example 1.1. We vary M to $\{3, 4, 5\}$ and use the MNIST benchmark to obtain training and testing instances. In Smallest Parent, training samples are of the form (x_1, x_2, p) , where x_1 and x_2 are CIFAR-10 images and p is the most immediate common ancestor of y_1 and y_2 , assuming the classes form a hierarchy. To simulate long-tail phenomena (denoted as **LT**), we vary the imbalance ratio ρ of the distributions of the input instances as in [4, 47]: $\rho = 0$ means that the hidden label distribution is unmodified and balanced. Each cell shows mean accuracy and standard deviation over three different runs. The results of our analysis are summarized in Table 1 and Table 2 (an extended version of Table 1 is in the appendix).

Table 1: Experimental results for MAX- M using $m_P = 3000$.

Algorithms	Original $\rho = 0$			LT $\rho = 15$			LT $\rho = 50$		
	$M = 3$	$M = 4$	$M = 5$	$M = 3$	$M = 4$	$M = 5$	$M = 3$	$M = 4$	$M = 5$
SL	84.15 ± 11.92	73.82 ± 2.36	59.88 ± 5.58	71.25 ± 4.48	66.98 ± 3.2	55.06 ± 5.21	66.74 ± 5.42	67.71 ± 11.58	55.74 ± 2.58
+ LA	84.17 ± 11.95	73.82 ± 2.36	59.88 ± 5.58	70.80 ± 4.52	66.98 ± 3.20	54.53 ± 5.74	66.57 ± 5.09	61.10 ± 3.95	52.47 ± 8.06
+ CAROT	84.57 ± 11.50	73.08 ± 3.10	60.26 ± 5.20	74.95 ± 3.45	67.44 ± 2.74	55.80 ± 4.47	68.16 ± 4.00	68.25 ± 6.14	57.29 ± 14.17
RECORDS	85.56 ± 7.25	75.11 ± 0.77	59.43 ± 6.61	55.47 ± 20.45	53.34 ± 16.66	52.40 ± 7.95	70.20 ± 7.65	66.05 ± 13.90	59.93 ± 4.86
+ LA	87.63 ± 5.11	75.11 ± 0.77	59.28 ± 6.76	54.90 ± 20.16	54.46 ± 15.54	51.25 ± 9.09	70.09 ± 7.26	65.78 ± 14.18	59.93 ± 4.86
+ CAROT	90.97 ± 2.03	75.94 ± 0.91	60.45 ± 7.78	54.32 ± 21.85	62.74 ± 8.14	55.85 ± 4.61	71.46 ± 6.4	71.25 ± 8.70	63.64 ± 5.92
LP(EMP)	94.97 ± 1.32	77.86 ± 4.22	55.27 ± 11.27	75.83 ± 5.26	69.67 ± 5.47	59.25 ± 7.27	77.16 ± 3.46	70.06 ± 10.73	56.79 ± 1.58
+ LA	94.69 ± 1.60	77.91 ± 4.16	55.34 ± 11.19	75.77 ± 5.32	68.92 ± 3.96	58.49 ± 5.74	77.1 ± 3.52	69.76 ± 10.31	56.81 ± 1.56
+ CAROT	95.07 ± 1.20	75.53 ± 7.42	53.07 ± 12.99	76.38 ± 4.72	69.74 ± 5.51	59.56 ± 8.14	77.58 ± 3.04	70.11 ± 10.34	57.09 ± 1.90
LP(ALG1)	96.09 ± 0.41	78.34 ± 4.80	59.91 ± 6.63	74.51 ± 9.13	69.14 ± 1.82	56.81 ± 3.74	72.23 ± 11.49	69.28 ± 11.78	63.67 ± 7.04
+ LA	95.81 ± 0.74	78.97 ± 4.09	59.98 ± 6.56	74.26 ± 9.06	68.73 ± 2.23	56.37 ± 3.13	72.23 ± 11.49	69.21 ± 11.86	63.67 ± 7.04
+ CAROT	96.13 ± 0.38	80.78 ± 2.36	59.71 ± 6.35	77.05 ± 7.00	69.19 ± 1.81	59.76 ± 7.24	74.82 ± 10.18	74.30 ± 7.54	64.39 ± 6.43

Table 2: Experimental results for Smallest Parent using $m_P = 10000$.

Algorithms	Original $\rho = 0$	LT $\rho = 5$	LT $\rho = 15$	LT $\rho = 50$	Algorithms	Original $\rho = 0$	LT $\rho = 5$	LT $\rho = 15$	LT $\rho = 50$
	SL	69.82 ± 0.53	67.94 ± 0.40	69.04 ± 0.03		74.65 ± 0.44	LP(EMP)	79.41 ± 1.33	79.24 ± 1.03
+ LA	69.83 ± 0.53	67.93 ± 0.41	68.70 ± 0.30	74.62 ± 0.36	+ LA	79.41 ± 1.33	79.24 ± 1.03	68.40 ± 1.90	70.29 ± 1.62
+ CAROT	69.82 ± 0.53	67.93 ± 0.41	68.70 ± 0.41	74.15 ± 0.47	+ CAROT	79.41 ± 1.33	79.28 ± 0.91	77.10 ± 1.74	80.71 ± 1.50
RECORDS	48.71 ± 3.90	48.15 ± 4.56	50.14 ± 1.10	55.12 ± 1.40	LP(ALG1)	80.23 ± 0.70	81.27 ± 0.71	81.99 ± 0.51	83.44 ± 0.48
+ LA	54.12 ± 2.00	45.48 ± 2.31	56.83 ± 1.30	60.87 ± 1.20	+ LA	80.20 ± 0.74	81.26 ± 0.72	81.99 ± 0.51	83.44 ± 0.48
+ CAROT	68.16 ± 0.47	69.04 ± 0.74	71.70 ± 0.84	75.69 ± 0.90	+ CAROT	68.90 ± 11.09	76.38 ± 5.68	82.00 ± 0.51	83.44 ± 0.48

Conclusions. Our empirical analysis reveals the following interesting phenomena: (i) training-time mitigation can significantly improve the accuracy; (ii) state-of-the-art on training-time mitigation might not appropriate for MI-PLL; (iii) approximate techniques for estimating r can sometimes be more effective when used for training-time mitigation; (iv) testing-time mitigation can substantially improve the accuracy of a model; however, it tends to be less effective than training-time mitigation; (v) CAROT may be sensitive to the quality of estimated ratios \hat{r} .

Regarding (i), let us focus on Table 2. We can see that both LP(EMP) and LP(ALG1) lead to higher accuracy than models trained exclusively via SL. For example, when $\rho = 5$ in Smallest Parent, the mean accuracy obtained via training under SL is 67.94%; the mean accuracy increases to 79.24% under LP(EMP) and to 81.27% under LP(ALG1). In MAX-4, the mean accuracy under SL is 55.48%, increasing to 78.56% under LP(ALG1). Regarding (ii), consider again Table 2. We can see that when RECORDS is applied jointly with SL, the accuracy of the model can substantially drop, e.g., when $\rho = 5$ in Table 2, the mean accuracy drops from 67.94% to 48.15%. In the MAX- M scenarios, RECORDS seems to improve over SL; however, for certain scenarios the accuracy drops drastically (e.g., for $\rho = 15$). The above stresses the importance of our LP-based technique.

Let’s now move to (iii). In most of the cases, LP(ALG1) leads to higher accuracy than LP(EMP). However, the opposite may also hold in some cases. One such example is the MAX-3 scenario, for $\rho = 50$: the mean accuracy for the baseline model is 66.74%, increasing to 72.23% under LP(ALG1) and to 77.16% under LP(EMP). A similar phenomenon is observed for $\rho = 15$ for the same scenario. This is an interesting phenomenon, as it suggests that there can be cases where employing the gold ratios (Algorithm 1 produces estimates that converge to the gold ratios, see Proposition C.1) may

not always be the best solution. A similar observation is done by the authors of RECORDS [13]. One cause of this phenomenon is the high number of classification errors observed during the initial stages of learning. Those classification errors can become higher in our experimental setting, as in the MAX- M scenarios, we only consider a subset of the pre-images of each partial label to compute SL and (7), in order to reduce the computational overhead of computing all pre-images.

We conclude with CAROT. Tables 1 and 2 show that CAROT can be more effective than LA. For example, in the MAX-3 scenarios and $\rho = 50$, the mean accuracy is 66.74% under SL, drops to 66.57% under SL+LA and increases to 68.16% under SL+CAROT. In Smallest Parent and $\rho = 50$, the mean accuracy of LP(EMP) increases from 70.29% to 80.71% under CAROT; LA has no impact. CAROT also improves the accuracy of RECORDS models, often, by a large margin. For example, for Smallest Parent and $\rho = 15$, the mean accuracy of a RECORDS-based trained model increases from 50.14% to 71.70% when CAROT is applied. CAROT is also consistently better than LA when applied on top of RECORDS. However, there can be cases where both LA and CAROT drop the accuracy of the baseline model. One such example is met in Smallest Parent and $\rho = 5$: the mean accuracy under LP(ALG1) is 81.27% and drops to 76.38% when CAROT is applied.

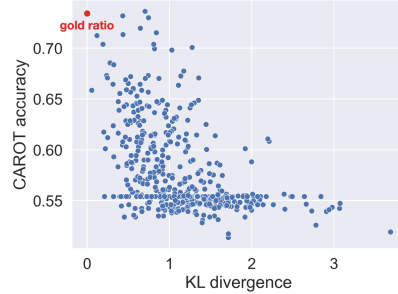


Figure 3: Impact of the label ratio quality on the performance of CAROT.

We analyse the sensitivity of CAROT under the quality of the input $\hat{\mathbf{r}}$, where quality is measured by means of the KL divergence to \mathbf{r} . Figure 3 shows the accuracy of an MNIST model (trained with the MAX-3 dataset), when CAROT is applied at testing-time using 500 randomly generated ratios $\hat{\mathbf{r}}$ of varying quality. We observe that CAROT’s effectiveness drops as the estimated marginal diverges more from \mathbf{r} . Also, the performance can decrease by more than 10% with only a small perturbation in the KL divergence. This instability may be the reason CAROT fails to improve a base model.

6 Related work

An extended version and more detailed comparison against the related work is in Appendix E.

Long-tail supervised learning. Two techniques on supervised learning that relate to our work are LA [28] and OTLM [31]. Both aim at testing-time mitigation. LA modifies the classifier’s scores by subtracting the gold ratios, i.e., via $\operatorname{argmax}_{y \in [c]} f^y(x) - \ln(r_y)$. CAROT can be substantially more effective than LA, see Section 5. OTLM assumes that the marginal \mathbf{r} is known, resorting to an OT formulation for adjusting the classifier’s scores. In contrast, we propose a statistically consistent technique to estimate \mathbf{r} , see Section 4.1, and resort to RSOT to accommodate for noisy $\hat{\mathbf{r}}$ ’s.

Long-tail PLL. Results showing that certain classes are harder to learn than others in standard PLL were presented in [7]. We are the first to extend those results for MI-PLL. The only two works in the intersection of long-tail learning and (single-instance) PLL are RECORDS [13] and SoLar [47]. Both aim at training-time mitigation. RECORDS modifies the classifier’s scores following the same idea with LA. It employs a momentum-updated prototype feature to estimate $\hat{\mathbf{r}}$. Differently from our LP-based technique, it does not take into account the constraints coming from MI-PLL. Section 5 shows that RECORDS is less effective than our proposed techniques, degrading the baseline accuracy on multiple occasions. On the other hand, SoLar relies on standard OT for assigning pseudo-labels to partially labelled instances, in contrast to our LP formulation (7). Also, SoLar uses a moving average technique to estimate \mathbf{r} , as opposed to Algorithm 1. See Section E for a detailed discussion on SoLar.

7 Conclusions

Our work is the first to theoretically characterize and mitigate learning imbalances in MI-PLL. Our theoretical characterization complements the existing theory in long-tail learning, identifying and addressing the unique challenges in MI-PLL. Additionally, we contributed an ILP-based and an RSOT-based mitigation technique that both outperform state-of-the-art in long-tail learning. Our empirical analysis unveiled two topics for future research: *computing marginal for testing-time mitigation* and *designing more effective testing-time mitigation techniques*. Another important future direction is to extend our theoretical analysis to more practical scenarios by dropping the i.i.d. assumption, which is the key to our label-specific bound formulation in Eq. (4).

References

- [1] Stephen Boyd and Lieven Vandenbergh. *Convex optimization*. Cambridge University Press, 2004.
- [2] Mateusz Buda, Atsuto Maki, and Maciej A. Mazurowski. A systematic study of the class imbalance problem in convolutional neural networks. *Neural Networks*, 106:249–259, 2018.
- [3] Vivien Cabannes, Alessandro Rudi, and Francis Bach. Structured prediction with partial labelling through the infimum loss. In *ICML*, page 1230–1239, 2020.
- [4] Kaidi Cao, Colin Wei, Adrien Gaidon, Nikos Arechiga, and Tengyu Ma. Learning imbalanced datasets with label-distribution-aware margin loss. In *NeurIPS*, pages 1567–1578, 2019.
- [5] Ming-Wei Chang, Lev Ratinov, and Dan Roth. Guiding Semi-Supervision with Constraint-Driven Learning. In *Proc. of the Annual Meeting of the Association for Computational Linguistics (ACL)*, pages 280–287, Prague, Czech Republic, 6 2007. Association for Computational Linguistics.
- [6] Nitesh V. Chawla, Kevin W. Bowyer, Lawrence O. Hall, and W. Philip Kegelmeyer. Smote: synthetic minority over-sampling technique. *Journal of Artificial Intelligence Research*, 16(1):321–357, 2002.
- [7] Timothee Cour, Ben Sapp, and Ben Taskar. Learning from partial labels. *Journal of Machine Learning Research*, 12:1501–1536, 2011.
- [8] Marco Cuturi. Sinkhorn distances: Lightspeed computation of optimal transport. In *NeurIPS*, 2013.
- [9] Wang-Zhou Dai, Qiuling Xu, Yang Yu, and Zhi-Hua Zhou. Bridging Machine Learning and Logical Reasoning by Abductive Learning. In *NeurIPS*, pages 2815–2826, 2019.
- [10] Kuzman Ganchev, João Graça, Jennifer Gillenwater, and Ben Taskar. Posterior regularization for structured latent variable models. *Journal of Machine Learning Research*, 11:2001–2049, 2010.
- [11] Nitish Gupta, Sameer Singh, Matt Gardner, and Dan Roth. Paired examples as indirect supervision in latent decision models. In *EMNLP*, pages 5774–5785, 2021.
- [12] Haibo He and Eduardo A. Garcia. Learning from imbalanced data. *IEEE Transactions on Knowledge and Data Engineering*, 21(9):1263–1284, 2009.
- [13] Feng Hong, Jiangchao Yao, Zhihan Zhou, Ya Zhang, and Yanfeng Wang. Long-tailed partial label learning via dynamic rebalancing. In *ICLR*, 2023.
- [14] Grant Van Horn and Pietro Perona. The devil is in the tails: Fine-grained classification in the wild. *CoRR*, abs/1709.01450, 2017.
- [15] Jiani Huang, Ziyang Li, Binghong Chen, Karan Samei, Mayur Naik, Le Song, and Xujie Si. Scallop: From probabilistic deductive databases to scalable differentiable reasoning. In *NeurIPS*, pages 25134–25145, 2021.
- [16] Robert I. Jennrich. Asymptotic properties of non-linear least squares estimators. *The Annals of Mathematical Statistics*, 40(2):633–643, 1969.
- [17] Rong Jin and Zoubin Ghahramani. Learning with multiple labels. In *NeurIPS*, pages 897–904, 2002.
- [18] Bingyi Kang, Saining Xie, Marcus Rohrbach, Zhicheng Yan, Albert Gordo, Jiashi Feng, and Yannis Kalantidis. Decoupling representation and classifier for long-tailed recognition. In *ICLR*, 2020.
- [19] Khang Le, Huy Nguyen, Quang M Nguyen, Tung Pham, Hung Bui, and Nhat Ho. On robust optimal transport: Computational complexity and barycenter computation. In *Advances in Neural Information Processing Systems*, pages 21947–21959, 2021.
- [20] Zenan Li, Yuan Yao, Taolue Chen, Jingwei Xu, Chun Cao, Xiaoxing Ma, and Jian Lu. Softened symbol grounding for neurosymbolic systems. In *ICLR*, 2023.
- [21] Tianyi Lin, Nhat Ho, Marco Cuturi, and Michael I. Jordan. On the complexity of approximating multimarginal optimal transport. *Journal of Machine Learning Research*, 23(1), 2022.

- [22] Wenpeng Liu, Li Wang, Jie Chen, Yu Zhou, Ruirui Zheng, and Jianjun He. A partial label metric learning algorithm for class imbalanced data. In *ACML*, volume 157, pages 1413–1428, 2021.
- [23] Jiaqi Lv, Miao Xu, Lei Feng, Gang Niu, Xin Geng, and Masashi Sugiyama. Progressive identification of true labels for partial-label learning. In *ICML*, page 6500–6510, 2020.
- [24] Robin Manhaeve, Sebastijan Dumancic, Angelika Kimmig, Thomas Demeester, and Luc De Raedt. Deepproblog: Neural probabilistic logic programming. In *NeurIPS*, pages 3749–3759, 2018.
- [25] Robin Manhaeve, Giuseppe Marra, and Luc De Raedt. Approximate Inference for Neural Probabilistic Logic Programming. In *KR*, pages 475–486, 2021.
- [26] Emanuele Marconato, Stefano Teso, Antonio Vergari, and Andrea Passerini. Not all neuro-symbolic concepts are created equal: Analysis and mitigation of reasoning shortcuts. In *NeurIPS*, 2023.
- [27] Stephen Mayhew, Snigdha Chaturvedi, Chen-Tse Tsai, and Dan Roth. Named Entity Recognition with Partially Annotated Training Data. In *Proc. of the Conference on Computational Natural Language Learning (CoNLL)*, 2019.
- [28] Aditya Krishna Menon, Sadeep Jayasumana, Ankit Singh Rawat, Himanshu Jain, Andreas Veit, and Sanjiv Kumar. Long-tail learning via logit adjustment. In *ICLR*, 2021.
- [29] Tsvetomila Mihaylova, Vlad Niculae, and André F. T. Martins. Understanding the mechanics of SPIGOT: Surrogate gradients for latent structure learning. In *EMNLP*, pages 2186–2202, 2020.
- [30] Mehryar Mohri, Afshin Rostamizadeh, and Ameet Talwalkar. *Foundations of Machine Learning*. The MIT Press, 2nd edition, 2018.
- [31] Hanyu Peng, Mingming Sun, and Ping Li. Optimal transport for long-tailed recognition with learnable cost matrix. In *ICLR*, 2022.
- [32] Hao Peng, Sam Thomson, and Noah A. Smith. Backpropagating through structured argmax using a SPIGOT. In *ACL*, pages 1863–1873, 2018.
- [33] Gabriel Peyré and Marco Cuturi. Computational optimal transport, 2020.
- [34] Aditi Raghunathan, Roy Frostig, John Duchi, and Percy Liang. Estimation from indirect supervision with linear moments. In *ICML*, volume 48, pages 2568–2577, 2016.
- [35] Dan Roth and Wen-tau Yih. *Global Inference for Entity and Relation Identification via a Linear Programming Formulation*. MIT Press, Introduction to Statistical Relational Learning edition, 2007.
- [36] Rajhans Samdani, Ming-Wei Chang, and Dan Roth. Unified expectation maximization. In *ACL*, pages 688–698, 2012.
- [37] Junghoon Seo and Joon Suk Huh. On the power of deep but naive partial label learning. In *ICASSP*, pages 3820–3824, 2021.
- [38] Shai Shalev-Shwartz and Shai Ben-David. *Understanding Machine Learning: From Theory to Algorithms*. Cambridge University Press, USA, 2014.
- [39] Vivek Srikumar and Dan Roth. The integer linear programming inference cookbook. *ArXiv*, abs/2307.00171, 2023.
- [40] Jacob Steinhardt and Percy S Liang. Learning with relaxed supervision. In *NeurIPS*, volume 28, 2015.
- [41] Jingru Tan, Xin Lu, Gang Zhang, Changqing Yin, and Quanquan Li. Equalization loss v2: A new gradient balance approach for long-tailed object detection. In *CVPR*, pages 1685–1694, June 2021.
- [42] Jingru Tan, Changbao Wang, Buyu Li, Quanquan Li, Wanli Ouyang, Changqing Yin, and Junjie Yan. Equalization loss for long-tailed object recognition. In *CVPR*, pages 11662–11671, 2020.
- [43] Efthymia Tsamoura, Timothy Hospedales, and Loizos Michael. Neural-symbolic integration: A compositional perspective. In *AAAI*, pages 5051–5060, 2021.
- [44] Grigori S Tseitin. On the complexity of derivation in propositional calculus. *Automation of reasoning*, 298:466–483, 1983.

- [45] Shyam Upadhyay, Ming-Wei Chang, Kai-Wei Chang, and Wen-tau Yih. Learning from explicit and implicit supervision jointly for algebra word problems. In *EMNLP*, pages 297–306, 2016.
- [46] A. W. van der Vaart. *Asymptotic Statistics*. Cambridge Series in Statistical and Probabilistic Mathematics. Cambridge University Press, 1998.
- [47] Haobo Wang, Mingxuan Xia, Yixuan Li, Yuren Mao, Lei Feng, Gang Chen, and Junbo Zhao. Solar: Sinkhorn label refinery for imbalanced partial-label learning. In *NeurIPS*, 2022.
- [48] Kaifu Wang, Hangfeng He, Tin D. Nguyen, Piyush Kumar, and Dan Roth. On Regularization and Inference with Label Constraints. In *ICML*, 2023.
- [49] Kaifu Wang, Efthymia Tsamoura, and Dan Roth. On learning latent models with multi-instance weak supervision. In *NeurIPS*, 2023.
- [50] Lei Wang, Dongxiang Zhang, Jipeng Zhang, Xing Xu, Lianli Gao, Bing Tian Dai, and Heng Tao Shen. Template-based math word problem solvers with recursive neural networks. In *AAAI*, pages 7144–7151, 2019.
- [51] Po-Wei Wang, Priya L. Donti, Bryan Wilder, and J. Zico Kolter. Satnet: Bridging deep learning and logical reasoning using a differentiable satisfiability solver. In *ICML*, 2019.
- [52] Hongwei Wen, Jingyi Cui, Hanyuan Hang, Jiabin Liu, Yisen Wang, and Zhouchen Lin. Leveraged weighted loss for partial label learning. *CoRR*, abs/2106.05731, 2021.
- [53] Jingyi Xu, Zilu Zhang, Tal Friedman, Yitao Liang, and Guy Van den Broeck. A semantic loss function for deep learning with symbolic knowledge. In *ICML*, pages 5502–5511, 2018.
- [54] Ning Xu, Congyu Qiao, Xin Geng, and Min-Ling Zhang. Instance-dependent partial label learning. In *NeurIPS*, volume 34, pages 27119–27130, 2021.
- [55] Zhun Yang, Adam Ishay, and Joohyung Lee. NeurASP: Embracing neural networks into answer set programming. In *IJCAI*, pages 1755–1762, 2020.
- [56] Peilin Yu, Tiffany Ding, and Stephen H. Bach. Learning from multiple noisy partial labelers. In *PMLR*, volume 151, pages 11072–11095, 2022.
- [57] Jieyu Zhang, Cheng-Yu Hsieh, Yue Yu, Chao Zhang, and Alexander J. Ratner. A survey on programmatic weak supervision. *ArXiv*, abs/2202.05433, 2022.
- [58] Yivan Zhang, Nontawat Charoenphakdee, Zheng Wu, and Masashi Sugiyama. Learning from aggregate observations. In *NeurIPS*, 2020.
- [59] Zhi-Hua Zhou. A brief introduction to weakly supervised learning. *National Science Review*, 5(1):44–53, 08 2017.

A Extended preliminaries

Optimal transport. Let Z_1 and Z_2 be two discrete random variables over $[m_1]$ and $[m_2]$. For $i \in [2]$, vector $\mathbf{b}^i \in \mathbb{R}_+^{m_i}$ denotes the probability distribution of Z_i , i.e., $\mathbb{P}(Z_i = m_j) = b_j^i$, for each $j \in [m_i]$. Let U be the set of matrices defined as $\{\mathbf{Q} \in \mathbb{R}_+^{m_1 \times m_2} \mid \mathbf{Q}\mathbf{1}_{m_1} = \mathbf{b}^2, \mathbf{Q}\mathbf{1}_{m_2} = \mathbf{b}^1\}$. The *optimal transport* (OT) problem [33] asks us to find the matrix $\mathbf{Q} \in U$ that maximizes a linear object subject to marginal constraints, namely

$$\min_{\mathbf{Q} \in U} \langle \mathbf{P}, \mathbf{Q} \rangle \quad (9)$$

Assume that we are strict in enforcing the probability distribution \mathbf{b}^1 , but not in enforcing \mathbf{b}^2 . The *robust semi-constrained optimal transport* (RSOT) problem [19] aims to find:

$$\min_{\mathbf{Q} \in U'} \langle \mathbf{P}, \mathbf{Q} \rangle + \tau \text{KL}(\mathbf{Q}\mathbf{1}_{m_1} \parallel \mathbf{b}^2) \quad (10)$$

where $U' = \{\mathbf{Q} \in \mathbb{R}_+^{m_1 \times m_2} \mid \mathbf{Q}\mathbf{1}_{m_2} = \mathbf{b}^1\}$ and $\tau > 0$ is a regularization parameter. In practice, the solution of (10) can be approximated in polynomial time using the *robust semi-Sinkhorn algorithm* that is proposed in [19], which generalizes the classical Sinkhorn algorithm [8] for OT.

B Proofs and details for Section 3

Proposition 3.1 (Class-specific risk bound). *For any $l_j \in \mathcal{Y}$, we have that $R_j(f) \leq \Phi_{\sigma, j}(R_{\mathcal{P}}(f; \sigma))$.*

Proof. This result directly follows from the definition of the program (4). \square

Proposition B.1. *Let $d_{[\mathcal{F}]}$ be the Natarajan dimension of $[\mathcal{F}]$. Given a confidence level $\delta \in (0, 1)$, we have that $R_j(f) \leq \Phi_{\sigma, j}(\tilde{R}_{\mathcal{P}}(f; \sigma, \mathcal{T}_{\mathcal{P}}, \delta))$ with probability $1 - \delta$ for any $j \in [c]$, where*

$$\tilde{R}_{\mathcal{P}}(f; \sigma, \mathcal{T}_{\mathcal{P}}, \delta) = \hat{R}_{\mathcal{P}}(f; \sigma, \mathcal{T}_{\mathcal{P}}) + \sqrt{\frac{2 \log(em_{\mathcal{P}}/2d_{[\mathcal{F}]}) \log(6Mc^2d_{[\mathcal{F]}}/e)}{m_{\mathcal{P}}/2d_{[\mathcal{F}]}) \log(6Mc^2d_{[\mathcal{F]}}/e)}} + \sqrt{\frac{\log(1/\delta)}{2m_{\mathcal{P}}}} \quad (11)$$

Proof. To start with, let $L_{\sigma} \circ [\mathcal{F}]$ be the function space that maps a (training) example (\mathbf{x}, s) to its partial loss:

$$L_{\sigma} \circ [\mathcal{F}] := \{(\mathbf{x}, s) \mapsto L_{\sigma}([f](\mathbf{x}), s) \mid f \in \mathcal{F}\} \quad (12)$$

The standard generalization bound with VC dimension (see, for example, Corollary 3.19 of [30]) implies that:

$$R_{\mathcal{P}}(f) \leq \hat{R}_{\mathcal{P}}(f; \mathcal{T}_{\mathcal{P}}) + \sqrt{\frac{2 \log(em_{\mathcal{P}}/d_{\text{VC}}(L_{\sigma} \circ [\mathcal{F}])))}{m_{\mathcal{P}}/d_{\text{VC}}(L_{\sigma} \circ [\mathcal{F}]})} + \sqrt{\frac{\log(1/\delta)}{2m_{\mathcal{P}}}} \quad (13)$$

where $d_{\text{VC}}(\cdot)$ is the VC dimension. For simplicity, let $d = d_{\text{VC}}(L_{\sigma} \circ [\mathcal{F}])$ and $d_{[\mathcal{F}]}$ be the Natarajan dimension of $[\mathcal{F}]$. Using a similar argument as in [49], given any d samples in $\mathcal{X}^M \times \mathcal{O}$ using $[\mathcal{F}]$, we let N be the maximum number of distinct ways to assign label vectors (in \mathcal{Y}^M) to these d samples. Then, the definition of VC-dimension implies that:

$$2^d \leq N \quad (14)$$

On the other hand, these d samples contain Md input instances in \mathcal{X} . By Natarajan's lemma (see, for example, Lemma 29.4 of [38]), we have that:

$$N \leq (Md)^{d_{[\mathcal{F}]}} c^{2d_{[\mathcal{F}]}} \quad (15)$$

Combining (15) with the above equations, it follows that

$$(Md)^{d_{[\mathcal{F}]}} c^{2d_{[\mathcal{F}]}} \geq N \geq 2^d \quad (16)$$

Taking the logarithm on both sides, we have that:

$$d_{[\mathcal{F}]} \log(Md) + 2d_{[\mathcal{F}]} \log c \geq d \log 2 \quad (17)$$

Taking the first-order Taylor series expansion of the logarithm function at the point $6d_{[\mathcal{F}]}$, we have:

$$\log(d) \leq \frac{d}{6d_{[\mathcal{F}]}} + \log(6d_{[\mathcal{F}]}) - 1 \quad (18)$$

Therefore,

$$\begin{aligned} d \log 2 &\leq d_{[\mathcal{F}]} \log d + d_{[\mathcal{F}]} \log M + 2d_{[\mathcal{F}]} \log c \\ &\leq d_{[\mathcal{F}]} \left(\frac{d}{6d_{[\mathcal{F}]}} + \log(6d_{[\mathcal{F}]}) - 1 \right) + d_{[\mathcal{F}]} \log M + 2d_{[\mathcal{F}]} \log c \\ &= \frac{d}{6} + d_{[\mathcal{F}]} \log(6Mc^2d_{[\mathcal{F}]} / e) \end{aligned} \quad (19)$$

Rearranging the inequality yields

$$\begin{aligned} d &\leq \frac{d_{[\mathcal{F}]} \log(6Mc^2d_{[\mathcal{F}]} / e)}{\log 2 - 1/6} \\ &\leq 2d_{[\mathcal{F}]} \log(6Mc^2d_{[\mathcal{F}]} / e) \end{aligned} \quad (20)$$

as claimed. \square

Proposition B.2. *If σ is M -unambiguous, then the risk of f can be bounded by*

$$R(f) \leq \sqrt{\mathbf{w}^\top (D(\Sigma_{\sigma, \mathbf{r}}))^\dagger \mathbf{w} R_{\mathcal{P}}(f; \sigma)} = \sqrt{c(c-1)R_{\mathcal{P}}(f; \sigma)} \quad (21)$$

which coincides with the Lemma 1 from [49] for $M = 2$.

Proof. As we discussed in the text, to find a loose bound of $R(f)$, we first define $\mathbf{w} := \sum_{i=1}^c r_i \mathbf{w}_i$ so that $R(f) = \mathbf{w}^\top \mathbf{h}$. Then, we consider the following relaxed program:

$$\begin{aligned} \max_{\mathbf{h}} \quad & \mathbf{w}^\top \mathbf{h} \\ \text{s.t.} \quad & \mathbf{h}^\top D(\Sigma_{\sigma, \mathbf{r}}) \mathbf{h} \leq R_{\mathcal{P}} \end{aligned} \quad (22)$$

where $D(\Sigma_{\sigma, \mathbf{r}})$ is the diagonal part of $\Sigma_{\sigma, \mathbf{r}}$, namely

$$D(\Sigma_{\sigma, \mathbf{r}}) = [r_i r_j \mathbb{1}\{i = j\} \mathbb{1}\{i \not\equiv j \pmod{c}\}]_{i \in [c^2], j \in [c^2]} \quad (23)$$

In other words, $D(\Sigma_{\sigma, \mathbf{r}})$ encodes all the partial risks that is caused by repeating the same type of misclassification twice. On the other hand, the M -unambiguity condition ensures that each type of misclassification, when repeated twice, leads to a misclassification of the partial label. Therefore, $\mathbf{w} \in \text{Range}(D(\Sigma_{\sigma, \mathbf{r}}))$.

The problem (22) is a special case of the single constraint quadratic optimization problem. Then, the fact that $\mathbf{w} \in \text{Range}(D(\Sigma_{\sigma, \mathbf{r}}))$ implies that the dual function of this problem (with dual variable λ) is

$$g(\lambda) = \lambda R_{\mathcal{P}} + \frac{\mathbf{w}^\top (D(\Sigma_{\sigma, \mathbf{r}}))^\dagger \mathbf{w}}{4\lambda} \quad (24)$$

where $(D(\Sigma_{\sigma, \mathbf{r}}))^\dagger$ is the pseudo-inverse, namely

$$(D(\Sigma_{\sigma, \mathbf{r}}))^\dagger = [(r_i r_j)^{-1} \mathbb{1}\{i = j\} \mathbb{1}\{i \not\equiv j \pmod{c}\}]_{i \in [c^2], j \in [c^2]} \quad (25)$$

Therefore,

$$\mathbf{w}^\top (D(\Sigma_{\sigma, \mathbf{r}}))^\dagger \mathbf{w} = c(c-1) \quad (26)$$

According to Appendix B of [1], strong duality holds for this problem. Therefore, the optimal value is given exactly as

$$\inf_{\lambda \geq 0} g(\lambda) = 2\sqrt{\frac{c(c-1)}{4} R_{\mathcal{P}}} = \sqrt{c(c-1)R_{\mathcal{P}}} \quad (27)$$

as claimed. \square

C Theoretical guarantees for Algorithm 1

The estimate $\hat{\mathbf{r}}$ given by Algorithm 1 can be viewed as a method to find the maximum likelihood estimation, whose consistency is guaranteed under suitable conditions. The most critical one is the invertibility of Ψ_σ . The invertibility is satisfied by practical transitions as the one from Example 1.1, but may fail to hold for certain transitions even if the M -unambiguity condition [49] holds. We will provide one such example later in this section.

Suppose our optimizer (the backpropagation step in Algorithm 1) can effectively find the maximum likelihood estimator. For a real $\epsilon > 0$, let Δ_c^ϵ be the shrunk probability simplex that is defined as $\{\mathbf{r} \in \Delta_c \mid r_j \geq \epsilon \forall j \in [c]\}$. Let $\hat{\mathbf{r}}_{m_p}^* := \operatorname{argmin}_{\hat{\mathbf{r}} \in \Delta_c^\epsilon} \sum_{j=1}^{c_S} \bar{p}_j \log[\Psi_\sigma(\hat{\mathbf{r}})]_j$ be the maximum likelihood estimation. We have that:

Proposition C.1 (Consistency). *If there exists an $\epsilon > 0$, such that $\mathbf{r} \in \Delta_c^\epsilon$ and Ψ_σ is injective in Δ_c^ϵ , then $\hat{\mathbf{r}}_{m_p}^* \rightarrow \mathbf{r}$ in probability as $m_p \rightarrow \infty$.*

Proof. Let $\Delta_{c_S}^{\sigma, \epsilon} := \{\Psi_\sigma(\mathbf{r}) \mid \mathbf{r} \in \Delta_c^\epsilon\}$ be the image of Ψ_σ on Δ_c^ϵ . The set $\Delta_{c_S}^{\sigma, \epsilon}$ is a compact subset in \mathbb{R}^{c_S} . For any partial label $a_j \in \mathcal{S}$, let $H(a_j, \mathbf{r}) := -\log([\Psi_\sigma(\mathbf{r})]_j)$ be the point-wise log-likelihood. The M -unambiguity condition ensures that each coordinate of every vector in $\Delta_{c_S}^{\sigma, \epsilon}$ should be at least ϵ^M , and hence the function H is bounded on $\Delta_{c_S}^{\sigma, \epsilon}$. By Theorem 1 of [16], this ensures that $\sum_s H(s, \mathbf{r})$ converges uniformly to $\mathbb{E}_S[H(S, \mathbf{r})]$. According to [46] (Theorem 5.7), the uniform convergence further ensures that $\Psi_\sigma(\hat{\mathbf{r}}_{m_p}^*) \rightarrow \mathbf{p}$ in probability as $m_p \rightarrow \infty$. Since Ψ_σ is invertible, this implies that $\hat{\mathbf{r}}_{m_p}^* \rightarrow \mathbf{r}$ in probability. \square

Counterexample where invertibility fails to hold. Consider the following transition function for binary labels ($\mathcal{Y} = \{0, 1\}$) and $M = 4$:

$$\sigma(y_1, y_2, y_3, y_4) = \begin{cases} 1, & \sum_{i=1}^4 y_i \in \{1, 2, 4\} \\ 0, & \text{otherwise} \end{cases} \quad (28)$$

The M -unambiguity condition [49] holds since $\sigma(0, 0, 0, 0) \neq \sigma(1, 1, 1, 1)$. On the other hand, the probability that the partial label equal to 1 can be expressed as:

$$\mathbb{P}(s = 1) = r_1^4 + 6r_1^2r_0^2 + 4r_1r_0^3 = r_1^4 + 6r_1^2(1 - r_1)^2 + 4r_1(1 - r_1)^3 \quad (29)$$

which is not an injection, as we can see from the plot of the function $t \mapsto t^4 + 6t^2(1 - t)^2 + 4t(1 - t)^3$ from below.

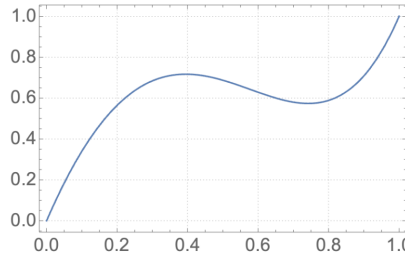


Figure 4: Plot of the function $t \mapsto t^4 + 6t^2(1 - t)^2 + 4t(1 - t)^3$.

D Details for Section 4.2

D.1 A non-linear program formulation

A straightforward idea that accommodates the requirements set in Section 4.2 is to reformulate (10) by firstly, extending \mathbf{P} (resp. \mathbf{Q}) to a tensor of size $n \times c \times M$ to store the scores (resp. pseudo-labels) of M -ary tuples of instances and secondly, modifying U' so that the combinations of entries in \mathbf{Q}

corresponding to invalid label assignments are forced to zero product. The pitfall is that modifying U' in this way does not allow us to employ Sinkhorn-like techniques as the one in [21], leaving us only with the option to employ non-linear¹ programming techniques to find \mathbf{Q} .

D.2 Deriving the linear program from (7)

Let $(x_{\ell,1}, \dots, x_{\ell,m}, s_{\ell})$ denote the ℓ -th partial training sample, where $\ell \in [n]$. For simplicity, we assume a single classifier f and use L to denote the size of the output domain. Each prediction is uniquely associated with a Boolean variable. In particular, we denote by $q_{\ell,i,j}$ the Boolean variable that becomes true if and only if $x_{\ell,i}$ is assigned with label j . Let $\mathbf{y}_{\ell,1}, \dots, \mathbf{y}_{\ell,R_{\ell}}$ denote the vectors of labels whose image under σ is s_{ℓ} , i.e., $\sigma(\mathbf{y}_{\ell,r}) = s_{\ell}$, for $r \in [R_{\ell}]$. Based on the above, each vector of labels $\mathbf{y}_{\ell,r}$ is associated with a conjunction of Boolean variables $\varphi_{\ell,r}$ from the set $\{q_{\ell,i,j} | i \in [m], j \in [L]\}$, while the training sample $(x_{\ell,1}, \dots, x_{\ell,m}, s_{\ell})$ is associated with the DNF formula $\Phi_{\ell} = \bigvee_{r=1}^{R_{\ell}} \varphi_{\ell,r}$. In the discussion that follows, we assume a canonical ordering over the variables occurring in $\varphi_{\ell,r}$ and use $\varphi_{\ell,r,j}$ to refer to the j -th variable and $|\varphi_{\ell,r}|$ to denote the number of (unique) variables occurring $\varphi_{\ell,r}$.

Our objective is to construct a linear program whose solutions capture the label assignments that abide by σ . In particular, the labels assigned to each $(x_{\ell,1}, \dots, x_{\ell,m})$ should be either of $\mathbf{y}_{\ell,1}, \dots, \mathbf{y}_{\ell,R_{\ell}}$. The construction of the linear program proceeds as in [39]. In particular, we first translate each Φ_{ℓ} into a CNF formula Φ'_{ℓ} . Then, out of each clause in Φ'_{ℓ} , we add the corresponding linear constraints.

Starting from $\Phi_{\ell} = \bigvee_{r=1}^{R_{\ell}} \varphi_{\ell,r}$, the first step of the Tseytin transformation associates a fresh Boolean variable $\alpha_{\ell,r}$ with each disjunction $\varphi_{\ell,r}$ in Φ_{ℓ} and introduces the constraint $\Lambda_{\ell,r} := \alpha_{\ell,r} \leftrightarrow \bigwedge_{j=1}^{|\varphi_{\ell,r}|} \varphi_{\ell,r,j}$, where $r \in [R_{\ell}]$. Recall that $\varphi_{\ell,r,j}$ refers to the j -th variable occurring in $\varphi_{\ell,r}$ and hence, it is a variable from $\{q_{\ell,i,j} | i \in [m], j \in [L]\}$. Then, Φ'_{ℓ} is logically equivalent to the formula:

$$\Phi'_{\ell} := \underbrace{\bigvee_{r=1}^{R_{\ell}} \alpha_{\ell,r}}_{\Psi_{\ell}} \wedge \bigwedge_{r=1}^{R_{\ell}} \Lambda_{\ell,r} \quad (30)$$

We proceed as follows. Similarly to [39], we will use the Iverson bracket to map Boolean variables to their corresponding integer ones, e.g., $[q_{\ell,i,j}]$, denotes the integer variable associated with the Boolean variable $q_{\ell,i,j}$.

The first inequality that will be added to the linear program corresponds to formula Ψ_{ℓ} . In particular, using Constraint (3) from [39], Ψ_{ℓ} is associated with the inequality $\sum_{r=1}^{R_{\ell}} [\alpha_{\ell,r}] \geq 1$. The next inequalities correspond to each $\Lambda_{\ell,r}$. Notice that $\Lambda_{\ell,r}$ can be written as the conjunction of formulas:

$$\alpha_{\ell,r} \rightarrow \bigwedge_{j=1}^{|\varphi_{\ell,r}|} \varphi_{\ell,r,j} \quad (31)$$

$$\bigwedge_{j=1}^{|\varphi_{\ell,r}|} \varphi_{\ell,r,j} \rightarrow \alpha_{\ell,r} \quad (32)$$

According to Constraint (10) from [39], (31) and (32) are associated with the following inequalities:

$$-|\varphi_{\ell,r}|[\alpha_{\ell,r}] + \sum_{j=1}^{|\varphi_{\ell,r}|} [\varphi_{\ell,r,j}] \geq 0 \quad (33)$$

$$-\sum_{j=1}^{|\varphi_{\ell,r}|} [\varphi_{\ell,r,j}] + [\alpha_{\ell,r}] \geq (1 - |\varphi_{\ell,r}|) \quad (34)$$

Lastly, according to Constraint (5) from [39], we have an equality $\sum_{j=1}^L [q_{\ell,i,j}] = 1$ for each $\ell \in [n], i \in [m]$, while we require each score $q_{\ell,i,j}$ to be in $[0, 1]$, for each $\ell \in [n], i \in [M], j \in [c]$.

¹Non-linearity comes from the KL term, as well as by enforcing invalid label combinations to have product equal to zero.

Putting everything together, we have the following linear program.

$$\begin{aligned}
\text{minimize} \quad & \min_{(\mathbf{Q}_1, \dots, \mathbf{Q}_m) \in \Delta^m} \sum_{i=1}^m \langle \mathbf{Q}_i, -\log(\mathbf{P}_i) \rangle, \\
\text{subject to} \quad & \sum_{r=1}^{R_\ell} [\alpha_{\ell,r}] \geq 1, & \ell \in [n], \\
& -|\varphi_{\ell,r}|[\alpha_{\ell,r}] + \sum_{j=1}^{|\varphi_{\ell,r}|} [\varphi_{\ell,r,j}] \geq 0, & \ell \in [n], r \in [R_\ell] \\
& -\sum_{j=1}^{|\varphi_{\ell,r}|} [\varphi_{\ell,r,j}] + [\alpha_{\ell,r}] \geq -1(1 - |\varphi_{\ell,r}|), & \ell \in [n], r \in [R_\ell] \\
& \sum_{j=1}^L [q_{\ell,i,j}] = 1, & \ell \in [n], i \in [m] \\
& [q_{\ell,i,j}] \in [0, 1], & \ell \in [n], i \in [M], j \in [c]
\end{aligned} \tag{35}$$

The program in Section 4.2 results after adding to the above program constraints coming from the marginal $\hat{\mathbf{r}}$.

E Extended related work

Long-tail learning. The term *long-tail learning* has been used to describe settings in which instances of some classes occur very frequently in the training set, with other classes being underrepresented. The problem has received considerable attention in the context of supervised learning with the proposed techniques operating either at training- or at testing-time. Techniques in the former category typically work by either reweighting the losses computed out of the original training samples [4, 42, 41] or by over- or under-sampling during training [6, 2]. Techniques in the latter category work by modifying the classifier’s output scores at testing-time and using the modified scores for classification [18, 31], with LA being one of the most well-known techniques [28]. LA modifies the classifier’s scores at testing-time by subtracting the (unknown) gold ratios. In particular, the prediction of classifier f given input x is given by $\arg \max_{y \in [c]} f^y(x) - \ln(r_y)$ under LA. Our empirical analysis shows that CAROT is more effective than testing-time mitigation techniques from the above line of research.

Closest to our work is the study in [31]. Differently from CAROT, the authors in [31] address with single-instance PLL and also assume that the marginal \mathbf{r} is known, using an optimal transport formulation [33] to adjust the classifier’s scores. In contrast, CAROT relies on the assumption that $\hat{\mathbf{r}}$ may be noisy, resorting to a robust optimal transport formulation [19] to improve the classification accuracy in those cases.

Partial Label Learning. As discussed in [49], MI-PLL is an extension to the standard, single-instance PLL. The observation that certain classes are harder to learn than others dates back to work of [7] in the context of PLL. Our work is the first to provide such results for MI-PLL, unveiling also the relationship between σ and class-specific risks.

Long-tail PLL. A few recently proposed papers lie in the intersection of long-tail learning and (single-instance) PLL, namely [22], RECORDS [13] and SoLar [47], with the first one focusing on non-deep learning settings. RECORDS modifies the classifier’s scores following the same basic idea with LA and uses the modified scores for training. However, it employs a momentum-updated prototype feature to estimate $\hat{\mathbf{r}}$. RECORDS’s design allows it to be used with any loss function and trivially be extended to support MI-PLL. Our empirical analysis shows that RECORDS is less effective than CAROT, leading to lower classification accuracy when the same loss is adopted to train the classifier.

SoLar shares some similarities with our LP formulation (7), as it also assigns pseudo-labels to the input instances at training-time based on the model’s prediction \mathbf{P} , in order to (strictly) match the marginal distribution $\hat{\mathbf{r}}$. In particular, given single-instance PLL samples of the form $\{(x_1, S_1), \dots, (x_n, S_n)\}$, where each $S_\ell \subseteq \mathcal{Y}$ is the partial label of the ℓ PLL sample², SoLar finds pseudo-labels \mathbf{Q} by solving the following linear program:

$$\begin{aligned}
& \min_{\mathbf{Q} \in \Delta} \langle \mathbf{Q}, -\log(\mathbf{P}) \rangle & (36) \\
\text{s.t.} \quad & \Delta = \{[q_{\ell j}]_{n \times L} \mid \mathbf{Q}^\top \mathbf{1}_n = \hat{\mathbf{r}}, \mathbf{Q} \mathbf{1}_c = \mathbf{c}, q_{\ell j} = 0 \text{ if } y_j \notin S_\ell\} \subseteq [0, 1]^{n \times c}
\end{aligned}$$

²In standard PLL, each partial label is a subset of classes from \mathcal{Y} .

The program (36) shows that the information of each partial label S_ℓ is strictly encoded into Δ . To directly extend (36) to MI-PLL, we have two options:

- Use an $n \times c^M$ tensor \mathbf{P} to store the model’s scores, where cell $P(\ell, j_1, \dots, j_c)$ stores the classifier’s scores for the label vector (j_1, \dots, j_c) associated with the ℓ -th training MI-PLL sample, for $1 \leq \ell \leq n$. However, that formulation would require an excessively large tensor, especially when M gets larger.
- Use separate tensors $\mathbf{P}_1, \dots, \mathbf{P}_M$ to represent the model’s scores of the M instances, and set for each $1 \leq \ell \leq n$, the product $P_1(\ell, j_1) \times \dots \times P_M(\ell, j_c)$ to be 0 if (j_1, \dots, j_c) does not belong to $\sigma^{-1}(s_\ell)$, where s_ℓ is the partial label of the ℓ -th training MI-PLL sample. However, that formulation would lead to a non-linear program.

Neither choice is scalable for MI-PLL when we have a large value of M^3 . To circumvent this issue, our work translates the information of the partial labels into linear constraints, leading to an LP formulation. Another difference between SoLar and work is that the ratio estimates $\hat{\mathbf{r}}$ can be obtained via Algorithm 1, while SoLar employs a window averaging technique to estimate \mathbf{r} based on the model’s own scores [47].

Finally, although our CAROT algorithm also use a linear programming formulation with a Sinkhorn-style procedure, it differs from SoLar in that it aims to adjust the model’s scores at testing time rather than assigning pseudo-labels at training time.

MI-PLL. There has been recently theoretical research on MI-PLL and related problems [26, 58, 49]. Differently from us, the work in [26] deals with the problem of characterizing *reasoning shortcuts* in MI-PLL. Intuitively, a reasoning shortcut is a classifier that has small partial risk, but high classification risk. For example, a reasoning shortcut is a classifier that may have a good accuracy on the overall task of returning the maximum of two MNIST digits, but low accuracy of classifying MNIST digits. The work has shown that current neurosymbolic learning techniques are vulnerable to learning reasoning shortcuts, proposing techniques to mitigate this phenomenon.

The authors in [49] were the first to propose necessary and sufficient conditions that ensure learnability of MI-PLL and to provide error bounds for a state-of-the-art neurosymbolic loss under approximations [15]. Our theoretical analysis extends the one in [49] by providing (i) class-specific risk bounds (in contrast to [49], which only bounds $R(f)$) and (ii) stricter bounds for $R(f)$. In particular, as we show in Proposition B.2, we can recover the error bound from Lemma 1 from [49] by relaxing (4).

Constrained learning. MI-PLL is closely related to constrained learning, in the sense that the prediction for the label (vector) is subject to the constraint $\sigma(\mathbf{y}) = s$ at the training stage. Training classifiers under constraints has been well studied in NLP [40, 34, 32, 29, 45, 50, 11]. The work in [35] proposes a formulation for training under linear constraints; [36] proposes a Unified Expectation Maximization (UEM) framework that unifies several constrained learning techniques including CoDL [5] and Posterior Regularization [10]. In particular, [27] employs a conceptually similar idea by encoding prior information of the label frequency with a CoDL formulation to enhance partial label learning for the Named Entity Recognition (NER) task. The UEM framework was also adopted by [20] for neurosymbolic learning. Our LP formulation is orthogonal to the UEM. These two could be integrated though.

It is also worth noting that a theoretical framework for constrained learning [48] provides generalization theory suggesting that encoding the constraint during both the training and testing stages results in a better model compared to encoding it only during the testing stage. This theory could potentially be extended to explain the advantage of LP-based methods and to characterize the necessary conditions for CAROT to improve model performance.

Neurosymbolic learning. MI-PLL quite often arises in neurosymbolic learning setting [24, 51, 9, 55, 43, 25, 15, 20]. However, none of the above lines of research deals with learning imbalances.

³Yet another non-linear formulation is presented in Section D based on RSOT (see Section A).

F Experimental details

Computational infrastructure. The experiments ran on an 64-bit Ubuntu 22.04.3 LTS machine with Intel(R) Xeon(R) Gold 6130 CPU @ 2.10GHz, 3.16TB hard disk and an NVIDIA GeForce RTX 2080 Ti GPU with 11264 MiB RAM. We used CUDA version 12.2.

Software packages. Our source code was implemented in Python 3.9. We used the following python libraries: scallopy⁴, highspy⁵, or-tools⁶, PySDD⁷, PyTorch and PyTorch Vision. Finally, we used part of the code⁸ available from [13] to implement RECORDS.

Classifiers. For the MAX- M scenarios, we used the MNIST CNN also used in [15, 24]. For the Smallest Parents scenarios, we used the ResNet model also used in [47, 13].

Further details. For the Smallest Parent scenarios, we computed SL and (7) using all the pre-image of each partial label. For the MAX- M scenarios, as the space of pre-images is very large, we only consider the top-1 proof [49] both when running Scallop and in (7).

For the Smallest Parent benchmark, we created the hierarchical relations shown in Listing 1 based on the classes of CIFAR-10.

Listing 1 Hierarchies for the Smallest Parent benchmark.

```
land_transportation :- automobile, truck
other_transportation :- airplane, ship
transportation :- land_transportation, other_transportation
home_land_animal :- cat, dog
wild_land_animal :- deer, horse
land_animal :- home_land_animal, wild_land_animal
other_animal :- bird, frog
animal :- land_animal, other_animal
entity :- transportation, animal
```

Table 3 presents the full results for the MAX- M scenarios.

⁴<https://github.com/scallop-lang/scallop> (MIT License).

⁵<https://pypi.org/project/highspy/> (MIT License).

⁶<https://developers.google.com/optimization/install/python> (Apache-2.0 license).

⁷<https://pypi.org/project/PySDD/> (Apache-2.0 license).

⁸<https://github.com/MediaBrain-SJTU/RECORDS-LTPLL> (MIT License).

Table 3: Experimental results for MAX- M using $m_P = 3000$.

Algorithms	Original $\rho = 0$			LT $\rho = 5$			LT $\rho = 15$			LT $\rho = 50$		
	$M = 3$	$M = 4$	$M = 5$	$M = 3$	$M = 4$	$M = 5$	$M = 3$	$M = 4$	$M = 5$	$M = 3$	$M = 4$	$M = 5$
SL	84.15 ± 11.92	73.82 ± 2.36	59.88 ± 5.58	55.48 ± 23.23	66.24 ± 1.22	55.13 ± 4.20	71.25 ± 4.48	66.98 ± 3.2	55.06 ± 5.21	66.74 ± 5.42	67.71 ± 11.58	55.74 ± 2.58
+ LA	84.17 ± 11.95	73.82 ± 2.36	59.88 ± 5.58	55.48 ± 23.23	65.63 ± 1.75	55.13 ± 4.20	70.80 ± 4.52	66.98 ± 3.20	54.53 ± 5.74	66.57 ± 5.09	61.10 ± 3.95	52.47 ± 8.06
+ CAROT	84.57 ± 11.50	73.08 ± 3.10	60.26 ± 5.20	56.52 ± 21.70	66.70 ± 0.76	55.91 ± 3.42	74.95 ± 3.45	67.44 ± 2.74	55.80 ± 4.47	68.16 ± 4.00	68.25 ± 6.14	57.29 ± 14.17
RECORDS	85.56 ± 7.25	75.11 ± 0.77	59.43 ± 6.61	77.98 ± 3.13	65.85 ± 0.62	55.07 ± 4.24	55.47 ± 20.45	53.34 ± 16.66	52.40 ± 7.95	70.20 ± 7.65	66.05 ± 13.90	59.93 ± 4.86
+ LA	87.63 ± 5.11	75.11 ± 0.77	59.28 ± 6.76	77.98 ± 3.13	65.43 ± 0.87	54.40 ± 4.44	54.90 ± 20.16	54.46 ± 15.54	51.25 ± 9.09	70.09 ± 7.26	65.78 ± 14.18	59.93 ± 4.86
+ CAROT	90.97 ± 2.03	75.94 ± 0.91	60.45 ± 7.78	78.31 ± 4.00	67.57 ± 1.74	55.46 ± 3.94	54.32 ± 21.85	62.74 ± 8.14	55.85 ± 4.61	71.46 ± 6.4	71.25 ± 8.70	63.64 ± 5.92
LP(EMP)	94.97 ± 1.32	77.86 ± 4.22	55.27 ± 11.27	80.15 ± 1.69	70.73 ± 1.85	56.28 ± 2.03	75.83 ± 5.26	69.67 ± 5.47	59.25 ± 7.27	77.16 ± 3.46	70.06 ± 10.73	56.79 ± 1.58
+ LA	94.69 ± 1.60	77.91 ± 4.16	55.34 ± 11.19	80.08 ± 1.55	70.54 ± 1.82	55.31 ± 3.27	75.77 ± 5.32	68.92 ± 3.96	58.49 ± 5.74	77.1 ± 3.52	69.76 ± 10.31	56.81 ± 1.56
+ CAROT	95.07 ± 1.20	75.53 ± 7.42	53.07 ± 12.99	80.29 ± 2.33	70.88 ± 2.22	57.85 ± 4.05	76.38 ± 4.72	69.74 ± 5.51	59.56 ± 8.14	77.58 ± 3.04	70.11 ± 10.34	57.09 ± 1.90
LP(ALG1)	96.09 ± 0.41	78.34 ± 4.80	59.91 ± 6.63	78.56 ± 1.52	69.71 ± 0.03	57.61 ± 3.09	74.51 ± 9.13	69.14 ± 1.82	56.81 ± 3.74	72.23 ± 11.49	69.28 ± 11.78	63.67 ± 7.04
+ LA	95.81 ± 0.74	78.97 ± 4.09	59.98 ± 6.56	78.48 ± 1.53	69.71 ± 0.03	57.47 ± 3.09	74.26 ± 9.06	68.73 ± 2.23	56.37 ± 3.13	72.23 ± 11.49	69.21 ± 11.86	63.67 ± 7.04
+ CAROT	96.13 ± 0.38	80.78 ± 2.36	59.71 ± 6.35	78.93 ± 1.85	70.32 ± 0.86	57.62 ± 3.08	77.05 ± 7.00	69.19 ± 1.81	59.76 ± 7.24	74.82 ± 10.18	74.30 ± 7.54	64.39 ± 6.43